Biochemistry and Biophysics Reports 5 (2016) 224–236

Contents lists available at ScienceDirect

Biochemistry and Biophysics Reports

journal homepage: www.elsevier.com/locate/bbrep

Identification of the phospholipid lysobisphosphatidic acid in the protozoan *Entamoeba histolytica*: An active molecule in endocytosis

Silvia Castellanos-Castro [a,c], Carlos M. Cerda-García-Rojas [b], Rosario Javier-Reyna [a], Jonnatan Pais-Morales [a], Bibiana Chávez-Munguía [a], Esther Orozco [a,*]

[a] Departamento de Infectómica y Patogénesis Molecular, Mexico
[b] Departamento de Química, Centro de Investigación y de Estudios Avanzados del IPN, Avenue IPN, 2508, CP 07360, D.F. México, México
[c] Colegio de Ciencia y Tecnología, Universidad Autónoma de la Ciudad de México, Dr. García Diego 168, CP 06720, D.F. México, México

ARTICLE INFO

Article history:
Received 1 July 2015
Received in revised form
25 November 2015
Accepted 21 December 2015
Available online 23 December 2015

Keywords:
Entamoeba histolytica
LBPA phospholipid
MVBs
Rab7
ALIX
Phagocytosis
EhADH

ABSTRACT

Phospholipids are essential for vesicle fusion and fission and both are fundamental events for *Entamoeba histolytica* phagocytosis. Our aim was to identify the lysobisphosphatidic acid (LBPA) in trophozoites and investigate its cellular fate during endocytosis. LBPA was detected by TLC in a 0.5 R_f spot of total lipids, which co-migrated with the LBPA standard. The 6C4 antibody, against LBPA recognized phospholipids extracted from this spot. Reverse phase LC-ESI-MS and MS/MS mass spectrometry revealed six LBPA species of *m*/*z* 772.58–802.68. LBPA was associated to pinosomes and phagosomes. Intriguingly, during pinocytosis, whole cell fluorescence quantification showed that LBPA dropped 84% after 15 min incubation with FITC-Dextran, and after 60 min, it increased at levels close to steady state conditions. Similarly, during erythrophagocytosis, after 15 min, LBPA also dropped in 36% and increased after 60 and 90 min. EhRab7A protein appeared in some vesicles with LBPA in steady state conditions, but after phagocytosis co-localization of both molecules increased and in late phases of erythrophagocytosis they were found in huge phagosomes or multivesicular bodies with many intraluminal vacuoles, and surrounding ingested erythrocytes and phagosomes. The 6C4 and anti-EhADH (EhADH is an ALIX family protein) antibodies and Lysotracker merged in about 50% of the vesicles in steady state conditions and throughout phagocytosis. LBPA and EhADH were also inside huge phagosomes. These results demonstrated that *E. histolytica* LBPA is associated to pinosomes and phagosomes during endocytosis and suggested differences of LBPA requirements during pinocytosis and phagocytosis.

1. Introduction

Entamoeba histolytica is the protozoan causative agent of human amoebiasis. It affects 50 million people around the world producing dysentery and liver abscesses [1]. Trophozoites are professional phagocytes and constitute the mobile and invasive phase of the parasite. Several proteins participating in phagocytosis have been identified, among them the Gal/GalNac lectin [2], EhC2PK, EhCaBP1, EhAK1 [3,4], several EhRab proteins [5–9] and the EhCPADH complex [10]. EhCPADH is formed by a protease (EhCP112) and an adhesin (EhADH) [10], a member of the ALIX family [11,12]. Lipids also influence the endosome membrane properties by changing biophysical characteristics and by recruiting proteins involved in membrane remodeling [13]. In addition, they protect trophozoites from the huge amount of endogenous proteases and amoebapore-forming proteins [14]. It has been reported that phosphoinositides are involved in the phagocytic cup formation, but not in the initial host cell interaction, neither at intermediate and late phases of phagocytosis and nor during pinocytosis [15,16]; though, earlier publications suggested that PI3-kinase inhibitors, diminish pinocytosis and parasite-host adherence [17]. Cholesterol is not synthesized by the parasite, even when it is essential for virulence expression [17,18]. Another intriguingly fact is that trophozoites have a higher ceramide proportion in comparison with mammalian cells [13,19]. However, the biological significance of this has not been fully elucidated.

In eukaryotes, plasma membrane invagination to trap the prey or cargo molecules is followed by endosomes and multivesicular bodies (MVBs) formation. In MVBs, some intraluminal vesicles (ILVs), carrying cargo molecules, are fused to other vesicles and lysosomes; whereas, vesicles carrying receptors are recycled to plasma membrane and other organelles [20]. Throughout

* Correspondence to: Departamento de Infectómica y Patogénesis Molecular, Avenue IPN 2508, Col. San Pedro Zacatenco, GAM, D.F. México, CP 07360, Mexico.
E-mail address: esther@cinvestav.mx (E. Orozco).

http://dx.doi.org/10.1016/j.bbrep.2015.12.010

maturation, endosomes modify pH, size, appearance and protein and lipids content [21,22]. The endosomal-sorting complex required for transport (ESCRT) and its accessory proteins, Alix and Vps4 ATPasa [23,24], participate in endocytosis. In addition, PI3P [25], PI(3,5)P_2 [26], cholesterol [27] and the phospholipid lysobisphosphatidic acid (LBPA), also named bis(monoacyl)glycerolphosphate(BMP) confer to the membranes specific characteristics to be remodeled during endocytosis [28,29].

Functional LPBA presents one fatty acid chain attached to the C2 of the two-glycerol backbones [30,31] and in general, its proportion of polyunsaturated acyl chains is higher than in other phospholipids [32–34]. LBPA is found mainly in acidic vesicles with high hydrolases content [35,36] and it is highly resistant to lipases and phospholipases. LBPA is present in animal tissues in a small amount, but it is enriched in vesicles inside late endosomes [37–39]. Using BHK cell membranes of late endosomes, Kobayashi et al. [38] generated a monoclonal antibody (6C4) against LBPA. LBPA is associated with Rab7, and interacts Alix, Niemann-Pick C (NPC) and saposin-C proteins during endocytosis. It participates in cholesterol distribution and homeostasis [28,37,38,40,41], sphingolipid metabolism [42], viral infection [43] and autoimmune diseases. Thus, LBPA is a critical component of endosomal/lysosomal network and it is essential for MVBs formation.

LBPA had not been identified in *E. histolytica* trophozoites. Here, we used the 6C4 antibody, reverse phase HPLC coupled to electrospray ionization mass spectrometry (ESI-MS) and tandem mass spectrometry (MS/MS) techniques, to reveal LBPA as a component of its phospholipid fraction. Our results demonstrated that LBPA is in endosomes during dextran uptake and erythrophagocytosis and it appeared associated to EhRab7A and EhADH proteins.

2. Materials and methods

2.1. Reference standards

(*S*,*S*)-2,2´-bisoleoyl-LBPA phospholipid standard was purchased from Echelon Bioscience in its lyophilized tetrabutylammonium salt.

2.2. Reagents

Dextran and FITC-dextran (mol wt 70,000) were from Sigma–Aldrich. Solvents for high performance liquid chromatography (HPLC) water (ChromAR®) and n-hexane (UltimAR®) were obtained from Macron Fine Chemicals. Anti-LBPA monoclonal antibodies (6C4 supernatant) were purchased from Echelon Bioscience. Secondary antibodies were purchased from Zymed and Invitrogen; anti-EhADH antibodies were generated in our group by immunizing rabbits twice each two weeks with 120 μg of a polypeptide corresponding to the EhADH C-terminus (566-QCVINLLKEFDNTKNI-582) coupled to the carrier protein Keyhole limpet hemocyanin (KLH), using TiterMax Classical Adjuvant (1:1 v/v) (Sigma-Aldrich). Anti-EhRab7A antibodies were kindly given by Dr. Tomoyoshi Nozaki [7].

2.3. E. histolytica cultures

Trophozoites of *E. histolytica* (strain HM1:IMSS) were axenically cultured in TYI-S-33 medium at 37 °C and harvested after 72 h [44]. Cell viability was monitored by optical microscopy and using Trypan blue dye exclusion test. Experiments presented here were performed at least three times in duplicate.

2.4. Lipids extraction procedure

Total lipids were extracted according to Folch [45]. Briefly, 120×10^6 trophozoites were placed in an extraction vial with 5 mL of methanol and incubated 20 min at 55 °C. Then, 2 volumes of chloroform were added and after sonication and vortexing, samples were incubated overnight (ON) at room temperature (RT). Samples were vortexed again, centrifuged for 10 min at 866*g* and filtered through a disc filter Whatman 1 M. Organic layer was collected, dried under liquid nitrogen and stored at −20 °C. An aliquot of total lipid extracts was used to determine phospholipids content [46].

2.5. Enzyme linked immunoassays (ELISA)

Wells of microtiter plates were coated with 0, 40 or 100 μg of trophozoites lipid extract dissolved in 100 μl of methanol:chloroform (98:2% v/v) and evaporated at RT. As a negative control, we added to other wells 40 or 100 μg of trophozoite proteins. As a positive control we employed 10 μg of (*S*,*S*)-2,2´-bisoleoyl-LBPA standard. Samples were blocked with 10% fetal bovine serum (FBS) in PBS and then, 10 μg/mL of 6C4 antibody (1:50) in PBS were added to the wells, which then, were incubated for 90 min at RT. Antibody was detected by anti-mouse horseradish peroxidase (HRP)-conjugated secondary antibody (1:3000), incubated for 1 h at RT and developed by *O*-phenylendiamine substrate (Zymed). Optical density (OD_{492}) was measured in a spectrophotometer (iMark, Biorad).

2.6. Thin layer chromatography (TLC)

Trophozoites lipid extracts were solubilized and spotted on TLC silica plates (Merck). Plates were developed by *n*-hexane:isopropanol:water (12:16:3 v/v/v) at RT for 6 h. Phospholipids were revealed by iodine vapors and they were identified by comparison with (*S*,*S*)-2,2´-bisoleoyl-LBPA standard spotted on the same silica plate. Solvent was removed using nitrogen flow.

2.7. Dot blot assays

Phospholipid fractions separated by TLC were scrapped off from the silica and dissolved in isopropanol/water (95:5%). Then, 50 μg of each one of the lipids extracted from the silica, 50 μg of LBPA and 50 μg of total lipid extracts from trophozoites were spotted on a polyvinylidene difluoride (PVDF) membranes. As a negative control we used lecithin and the secondary antibody on total lipids. Lipid spots were dried and filters were blocked with 10% FBS in PBS, ON at 4 °C. Membranes were then incubated for 3 h at RT with 6C4 antibody (1:100), washed four times with PBS-Tween 20, (0.02%) and revealed with HRP-conjugated anti-mouse antibody (1:9000). After washing several times with PBS-Tween 20, reactivity was visualized using a commercial enhanced chemiluminescence imaging system MicroChem 4.2 (Bio Imaging System).

2.8. High-performance liquid chromatography (HPLC) analysis

Samples of total lipids were dissolved in methanol. Reverse-phase HPLC was performed according to Mortuza et al. [34] using an Agilent 1 200 capillary LC pump chromatograph. Phospholipid elution was carried out using a binary system as follows: Eluent A: 0.25% (v/v) ammonium hydroxide/0.05% (v/v) formic acid in methanol, pH 6.4:water (88:12). Eluent B: 0.25% (v/v) ammonium hydroxide/0.05% (v/v) formic acid in methanol, pH 6.4:hexane (80:20). All mobile phases were freshly prepared, filtered through 0.22 μm filter (Millipore) and degassed under vacuum. Samples

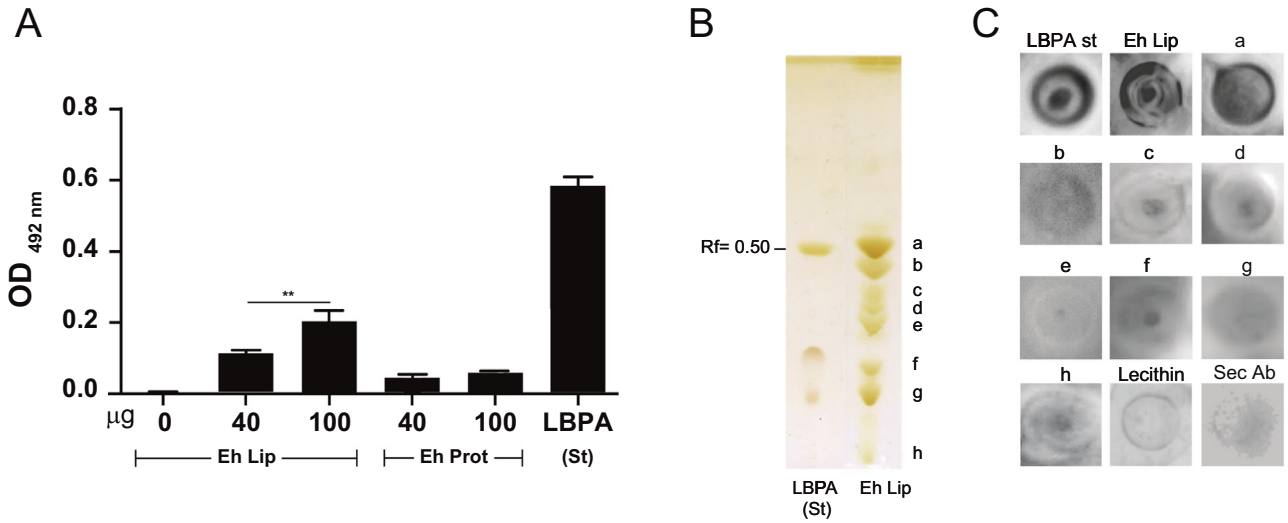

Fig. 1. Immunodetection of LBPA in *E. histolytica* trophozoites. (A) ELISA assays revealed by 6C4 antibody and HRP-labeled secondary antibodies. Eh Lip: between 40 and 100 µg of trophozoites total lipids. Data are means ± standard deviation. (**): $p < 0.01$. Eh Prot: 40 and 100 µg of trophozoites total proteins. LBPA (St): 10 µg of (*S, S*)-2,2´-bisoleoyl-LBPA. (B) TLC revealed by iodine vapors. Letters at the right mark each one of the separated phospholipids. (C) Dot blots assays revealed by 6C4 antibody followed by HRP-labeled secondary antibody: LBPA St: (*S,S*)-2,2´-biosoleoyl-LBPA standard (10 µg); Eh Lip: Total lipids extracts of *E. histolytica* (50 µg); a-h: phospholipids extracted from (B) (50 µg each); Lecithin: (50 µg); Sec Ab: secondary antibody on total lipids.

were injected on a Zorvax SB C18 HPLC column (5 µm, 150 × 0.5 mm^2). A linear gradient was performed by increasing eluent B from 25 to 75% during 42 min with a flow rate of 10 µL/min. As a standard reference we used (*S,S*)-2,2´-bisoleoyl-LBPA.

2.9. Mass spectrometry (MS) analysis

MS data were acquired using a triple quadrupole spectrometer with lineal ion trap 3200 Q-Trap (Applied Biosystem Instruments). Mass spectrometric data analysis was performed in a negative-ion mode using an ionizing turbo spray source. During electrospray mass-spectrometry (ESI-MS) run, averages of 155 scans were continuously saved. Elution range of LBPA was determined based on elution of (*S,S*)-2,2´-bisoleoyl-LBPA standard. *E. histolytica* LBPA molecular species were identified using information dependent acquisition (IDA) method, which included a survey scan in enhanced mass spectrometry (EMS) and MS/MS. The EMS scan was carried out at a rate of a spectral range *m/z* 700–900, and energies to perform ion fragmentation were optimized with the standard. Relative quantities of molecular species were obtained from their mass spectral intensities.

2.10. Transmission electron microscopy (TEM) assays

Trophozoites were fixed with 4% PFA and 0.5% glutaraldehyde in PBS for 1 h at RT. Samples were embedded in LR White resin (London Resin Co) and polymerized under UV at 4 °C ON. Thin sections (0.5 µm) were obtained and mounted on formvar-covered nickel grids. Later, they were incubated ON with 6C4 antibody (1:10) and then, cells were incubated ON at RT with goat anti-mouse IgG conjugated to 20 nm gold particles (Ted Pella Inc.) (1:40). Thin sections were observed with a Jeol JEM-1011 transmission electron microscope. For phagocytosis experiments, trophozoites were first incubated with human erythrocytes (1:50 ratio) at 37 °C for 0–120 min and treated for TEM as described above. Number of gold particles was counted in 64 µm^2 of distinct images of at least 12 different thin sections.

2.11. Immunofluorescence and endocytosis assays

Trophozoites were grown on coverslips during 72 h at 37 °C in TYI-S-33 medium and fixed with 4% paraformaldehyde (PFA) (Sigma) at RT for 1 h. Cells were permeabilized with 0.02% saponin (Sigma) in PBS for 10 min at RT and blocked for 30 min with 0.2% FSA diluted in PBS. Then, trophozoites were incubated with 6C4 antibody (1:30) ON at 4 °C, washed with PBS and then, incubated during 1 h at RT with anti-mouse Alexa-594 labeled secondary antibody (Invitrogen) (1:100). After washing with PBS, preparations were preserved using the Vectashield reagent (Vector Lab) and analyzed through a Nikon inverted microscope attached to a laser confocal scanning system (Leica TCS_SP5_MO). For co-localization experiments, cells were double-labeled with anti-Rab7A (1:500) [7] or anti-EhADH (1:500) and 6C4 antibodies followed by anti-rabbit FITC labeled secondary and anti-mouse Alexa-594 labeled secondary antibodies, respectively. For endocytosis assays, trophozoites were incubated at 37 °C with 2 mg/mL of FITC-dextran (mol wt 70,000) (Sigma-Aldrich), or with erythrocytes (1:50 ratio) for different times (0–90 min). After incubation times, erythrocytes were contrasted by diaminobezidine for better visualization [47]. Cells were fixed, permeabilized and processed for immunofluorescence assays as described above, using 6C4 and anti-EhADH antibodies and Lysotracker. For Lysotracker labeling assay, cultures were incubated in TYI-S-33 medium supplemented with 2 µg/mL of Lysotracker Red (Invitrogen) for the last 2 h of incubation. Trophozoites were washed three times with PBS and then, samples were processed for immunofluorescence as described above.

2.12. Quantification of fluorescence

Confocal microscopy images were analyzed with Image J 1.48i software [48]. To quantify the fluorescence intensity inside the cell, we used images of maximum projections. The region around each cell was drawn and the cellular area, the integrated intensity and the mean gray values were measured. Measurements of other regions without fluorescence were used for background subtraction. The net average fluorescence intensity per pixel, expressed as corrected total cell fluorescence (CTCF), was calculated for each trophozoite and time point with the formula [49,50]:

CTCF = Whole cell signal − (area of selected cell × fluorescence of background). Where whole cell signal = sum of pixels intensity for each cell (integrated intensity value). Fluorescence of background = average signal per pixel for a region without fluorescence selected just beside the cell (mean gray value).

To quantify stained pinosomes and phagosomes, as well as Lysotracker stained vesicles, 1-µm Z-stacks of whole cell were

acquired. To calculate the relative percentages of merging vesicles during pinocytosis, the number of FITC-dextran stained pinosomes was considered as 100% at each time, then, percentages of merging pinosomes were obtained. For quantification of LBPA in phagocytic trophozoites, the number of ingested erythrocytes was taken as 100%, then, the percentage of 6C4 of stained phagosomes was calculated. For triple labeling experiments, 6C4, anti-EhADH, Lysotracker and merging stained vesicles with or without erythrocytes was calculated taking as 100% the 6C4 stained vesicles. To determine co-localization in entire cell or an area around merging vesicles, merging channels of 1-μm Z-stacks ($n=150$ sections) were contrasted, then, colors were separated to be analyzed using the Just Another Co-localization Plugin (JACoP) in the ImageJ 1.48i software [51] to calculate Pearson´s coefficient (PC). Each point represented an average and values are given as means ± standard deviation.

2.13. Immunoprecipitation assays

Trophozoites in steady state conditions or after 90 min of erythrophagocytosis using hemoglobin-depleted and Ficoll-1077 (Sigma-Aldrich) [52,53] purified erythrocytes were lysed with 10 mM Tris–HCl, and 50 mM NaCl, NaH_4Cl, $NaHCO_3$ in the presence of protease inhibitors (100 mM of PHMB, IA, NEM and TLCK), followed by freeze-thawing cycles in liquid nitrogen and vortexing. In parallel, 200 μl of recombinant protein G (rProtein-G) agarose (Invitrogen) were incubated with 100 μg of rabbit anti-EhADH antibodies, or 6C4 monoclonal antibody or pre-immune serum (PS) for 2 h at 4 °C, with gentle stirring. Then, rProtein-G beads were washed with 0.5% BSA in PBS under gentle stirring and centrifuged at 11,600 g for 2 min. Trophozoites lysates (1 mg) were pre-cleared with 200 μl of rProtein-G (previously blocked with 2% BSA) and incubated 2 h at 4 °C under gentle stirring. Samples were centrifuged at 11,600g to obtain the supernatant that was added to rProtein-G previously incubated with antibodies. Samples were incubated ON at 4 °C and then, beads were recovered by centrifugation. After washing, samples were dotted on a nitrocellulose membrane to detect the phospholipid and EhADH protein by dot blot assays. As a positive control we used 10 μg of LBPA standard, and as negative control, we performed immunoprecipitation assays using 6C4, anti-EhADH antibodies and erythrocytes lysates. To avoid heavy chains signals, blots were incubated with light chain specific secondary antibodies (1:10,000) (Jackson ImmunoResearch). Western blot assays of immunoprecipitates were performed to confirm the identity of proteins detected by dot blot experiments incubating membranes with 12% SDS-PAGE separated proteins ON with anti-EhADH antibody (1:500), followed by incubation with anti-rabbit HRP-conjugated antibody (1:9000) in PBS, during 1 h at RT.

2.14. Statistics

Graphs and statistical analysis were performed using GraphPad Prism 6 software Inc. Each point represented an average of 12–25 cells and values are given as means ± standard deviation. Student´s T statistics analyses were performed comparing the values of each time tested to the first kinetics time measured. $p > 0.05$ values were not considered as statistically representative. $p < 0.05$ (*), $p < 0.01$ (**) were considered as statistically representative and $p < 0.001$ (***) values were considered as highly significant.

3. Results

3.1. Lbpa is present in E. Histolytica trophozoites

To disclose the presence of LBPA in total lipids of *E. histolytica* trophozoites, we carried out ELISA assays using the 6C4 monoclonal antibody [38]. The antibody recognized total lipids of trophozoites in a dose dependent manner as well as the (*S*, *S*)-2,2´-bisoleoyl-LBPA standard control (Fig. 1 A). However, it did not react with total proteins of trophozoites, neither with the uncoated wells (Fig. 1 A). These results suggested that LBPA is present in total lipids of *E. histolytica*.

Phospholipids separated by TLC from total lipids of *E. histolytica* and revealed by iodine vapors showed eight spots (Fig. 1B, A–H). The bottom of the spot labeled with letter “a” co-migrated with the LBPA standard at a 0.50 R_f band (Fig. 1B), suggesting that *E. histolytica* LBPA could be located in this spot. To confirm this, we carefully extracted from preparative plates the phospholipids in each lane with distinct R_f, to carry out dot blot assays using the 6C4 antibody. Antibody recognized phospholipids extracted from spot “a” (R_f 0.50), total lipid extracts of trophozoites and the LBPA standard, but not phospholipids from other spots obtained from TLC plates and nor with lecithin. The secondary antibody on total lipids gave also negative results (Fig. 1C). These results strongly suggested that the bottom of spot “a” contained *E. histolytica* LBPA.

3.2. There are at least six different molecular species of LBPA in E. histolytica trophozoites

To confirm the identity of *E. histolytica* LBPA, we performed reverse phase LC-ESI and MS/MS analysis. Total ion chromatogram (TIC) profiles were determined using information dependent acquisition (IDA) experiments to define the retention of (*S*,*S*)-2,2´-bisoleoyl-LBPA standard, which eluted mainly at 24.57 min (Fig. 2A). LC-ESI-MS spectra of the elution peak evinced a molecular ion with *m/z* 773.58 (Fig. 2B), which is in agreement with reports of other authors [34]. Spectra of LC-ESI-MS phospholipids extracted from spot “a” ($R_f = 0.5$) and from the total lipid fraction that eluted at the same time that the standard, were similar. They presented at least six ions distributed in two groups corresponding to closely related molecular species: *m/z* 772.58, 774.48 and 776.58 (group I) and *m/z* 798.72, 800.76 and 802.68 (group II) (Fig. 2C). Ion identity was confirmed upon ion fragmentation by MS/MS. (*S*,*S*)-2,2´-biosoleoyl-LBPA standard produces ions corresponding to oleic acid: *m/z* 281, phosphate moiety: *m/z* 79, glycerolphosphate: *m/z* 153, and this ion is considered as a diagnostic ion of LBPA [34] (Fig. 2D and E). Ion *m/z* 153 was detected in MS/MS spectra of the six ions identified in *E. histolytica* by LC-ES-MS. Fig. 2F shows the ion fragmentation of *E. histolytica* LBPA, containing 18:1/18:1 (*m/z* 774.48) fatty acids as representative example. Relative abundance of these components was calculated from their mass spectral intensities (Table 1). The major *E. histolytica* LBPA molecular species was 38:3 (18:1/20:2) corresponding to 43% of total LBPA. The majority of the fatty acids found in these species were unsaturated, being 18:1 and 20:2 the most abundant (Table 1). These experiments confirmed the *E. histolytica* LBPA identity and composition.

3.3. LBPA is located in cytoplasm and vesicles

To investigate the cellular location of LBPA in trophozoites, we performed TEM using the 6C4 monoclonal antibody and gold-labeled secondary antibodies. In steady sate conditions (0 time, without phagocytosis or pinocytosis stimuli), TEM images displayed LBPA distributed in the cytoplasm and in many vacuoles of different size (Fig. 3A–D). Number of gold labeled particles in TEM images showed that a mean of 71.8% of total *E. histolytica* LBPA particles were located in vesicles, whereas 28.2% were in the cytoplasm (Fig. 3B).

3.4. During dextran uptake, LBPA co-localizes with cargo-carrying pinosomes.

To investigate the association of LBPA with endosomes during pinocytosis, we carried out experiments incubating trophozoites with

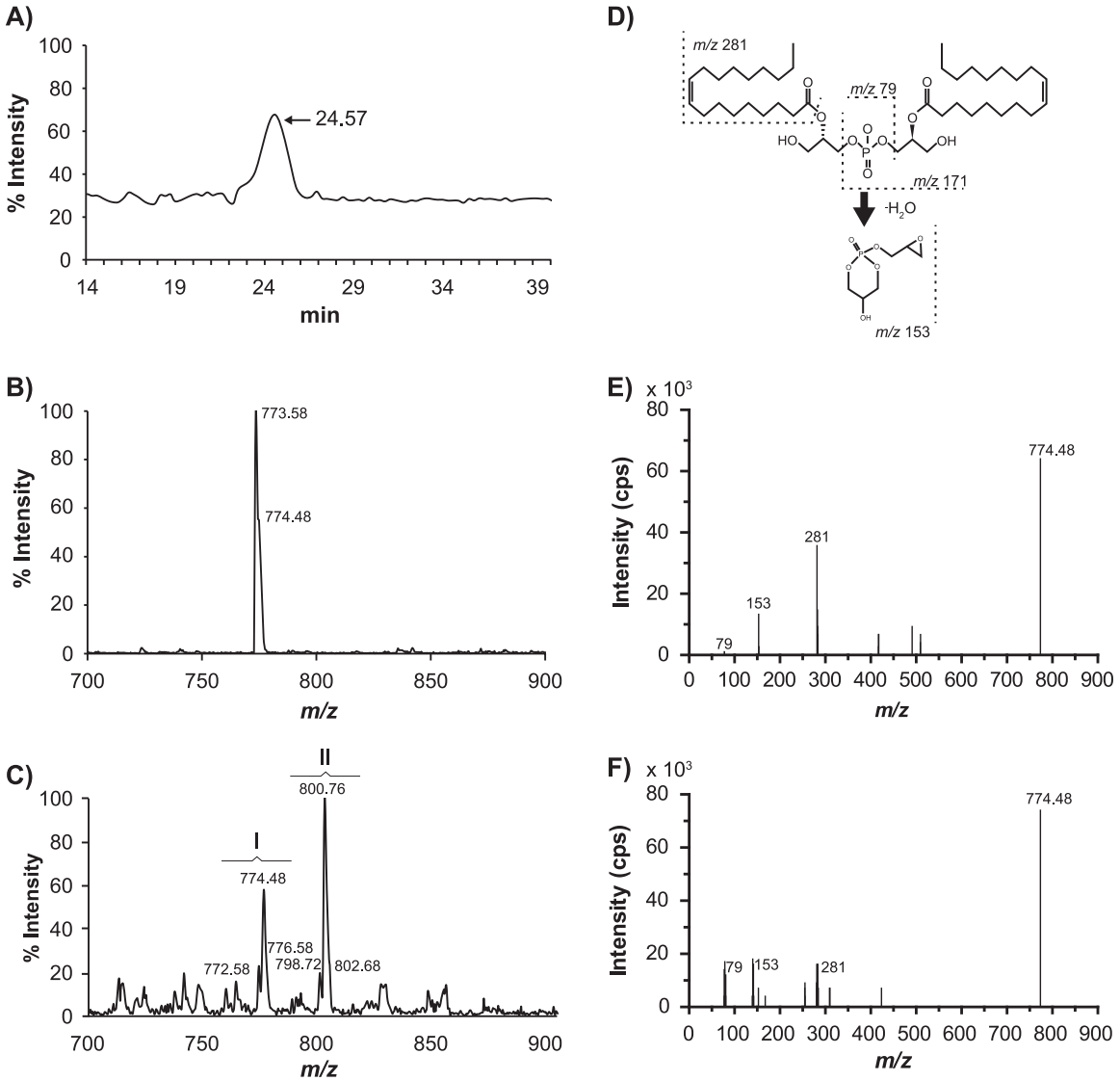

Fig. 2. LC-ESI-MS spectra of *E. histolytica* LBPA. (A) TIC of (*S,S*)-2,2´-bisoleoyl-LBPA standard obtained by LC analysis. Arrow marks the retention time. (B) LC-ESI-MS spectra of (*S,S*)-2,2´-bisoleoyl-LBPA standard. (C) LC-ESI-MS spectra of *E. histolytica* phospholipids eluted from 24 to 25 min. I and II: groups of LBPA molecular species, numbers show the *m/z* of LBPA species. (D) Structure of *(S-S)*-2,2´-bisoleoyl-LBPA. Numbers indicate *m/z* of ion products upon fragmentation. (E) Spectra of *(S-S)*-2,2´-bisoleoyl-LBPA fragmentation. (F) MS/MS spectra of *m/z* 774.48 *E. histolytica* LBPA ion.

Table 1
Molecular species of LBPA in *E. histolytica*.

Molecular ion	*m/z*	Subclass	Molecular species	Relative abundance
1	772.58	36:3	18:1/18:2	10
2	774.48	36:2	18:1/18:1	25
3	776.58	36:1	18:1/18:0	4
4	798.72	38:4	18:0/20:4	8
5	800.76	38:3	18:1/20:2	43
6	802.68	38:2	18:1/20:1 (18:0/20:2)	11

FITC-dextran from 0 to 120 min and after cell fixation with the 6C4 followed by Alexa-594 secondary antibodies, and then, they were examined through the confocal microscope (Figs. 4 and 5). Intriguingly, after 15 min of pinocytosis, fluorescence corresponding to 6C4-Alexa-594 antibodies, calculated by CTCF, drastically diminished in 84% (6.3 fold) in comparison with steady state conditions (Fig. 5A). Then, after 60 min, 6C4 fluorescence came back to levels close to those showed by trophozoites in steady state conditions, reaching a plateau at 60 min (Fig. 5A). According to other authors [54], drastic diminish of LBPA immediately after beginning of endocytosis is due to the fact that the pool of certain lipids, including LBPA, is used by the cell to synthesize other metabolites but the reasons of these changes remain to be studied in *E. histolytica*. During pinocytosis, some vesicles were decorated only by FITC-dextran, or by 6C4 antibody or both (Figs. 4, 5B). Thus, the relative percentage of LBPA containing pinosomes that merged with FITC-dextran was quantified, taken as 100% the number of FITC-labeled vesicles at each time (Fig. 5B). At 15 min of pinocytosis, we detected 33.84% of vesicles stained by FITC and Alexa 594, at 30 min, merging vesicles corresponded to 47.2%, at 60 min to 49.5%, and at 120 min to 56.6%, reaching a plateau (Fig. 5B). In agreement with Aley et al. [55], the plateau means that equilibrium between dextran uptake and excretion has been reached [54]. These results showed that the number of LBPA and FITC-dextran containing vesicles varied through the time course of pinocytosis. Pearson's coefficients indicated that association between FITC-dextran and LBPA inside the trophozoites varied from 0.61 to 0.70 (Fig. 5C).

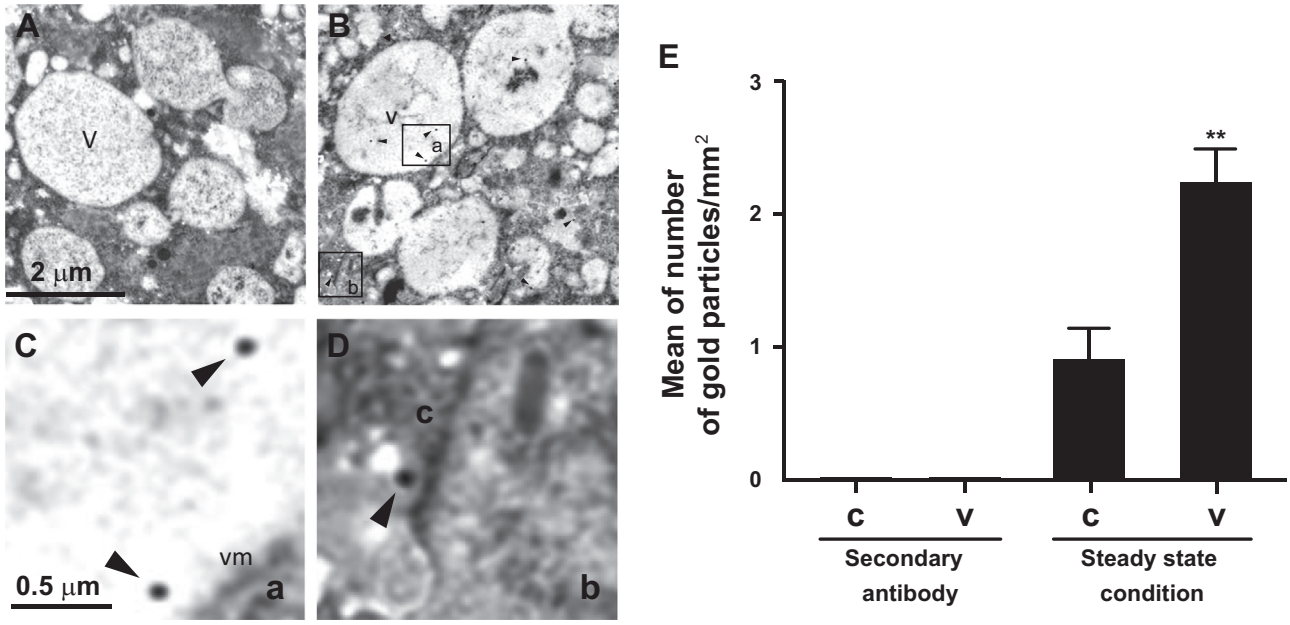

Fig. 3. Immunolocalization of LBPA in trophozoites in steady state conditions. (A) Assays were performed using only the secondary antibody. (B) TEM of thin sections of trophozoites treated with 6C4 antibody and gold-labeled secondary antibody. (C) Magnification of square (a) showing a part of a vesicle. (D) Magnification of square (b) showing a part of the cytoplasm. Arrowheads: gold particles. (E) Number of gold particles in (c): cytoplasm, (v): vesicles. Secondary antibodies: Experiments performed using only the secondary antibody. Data are means ± standard deviation. (**): $p < 0.01$.

3.5. During phagocytosis, LBPA is located in erythrocytes-containing phagosomes

Phagocytosis of bacteria and erythrocytes is a nutrition way for *E. histolytica* trophozoites, and erythrophagocytosis is considered as a virulence factor. Therefore, we performed erythrophagocytosis assays at different times to study the LBPA distribution in trophozoites (Figs. 6 and 7). After 15 min of phagocytosis, in TEM images, using 6C4 antibody and gold-labeled secondary antibodies, 2.1 gold particles/μm^2 appeared in membranes of erythrocyte-containing phagosomes and 1.5 gold particles/μm^2, inside the erythrocytes (Fig. 6A–C). However, at longer times (90 min), gold particles/μm^2 that were located in phagosome membranes, diminished from 2.1 to 1.5 particles/μm^2, but they increased 11 fold inside phagosomes (Fig. 6C). Interestingly, at 90 min, LBPA containing vesicles appeared accumulated around erythrocytes (Fig. 6B). However, even when this fact could suggest that they are carrying LBPA to phagosomes, it is necessary to perform other functional assays to prove this. Quantification assays exhibited that LBPA in vesicles without erythrocytes increased twice throughout the erythrophagocytosis process, from 2.7 at 0 time to 5.5 gold particles/μm^2 at 90 min (Fig. 6B,C).

Confocal microscopy images obtained between 0 and15 min of phagocytosis, confirmed that LBPA was accumulated in vesicles close to ingested erythrocytes inside phagosomes of different size (some of them, containing more than one erythrocyte and numerous vacuoles) and on erythrocytes. From 60 to 90 min of phagocytosis, LBPA appeared mainly on and around erythrocytes-containing phagosomes (Fig. 7), although many erythrocytes appeared already digested. This was more evident in huge phagosomes (10–20-μm diameters) that could correspond to MVBs. These structures contained many putative ILVs. Magnification of erythrocytes-containing phagosomes demonstrated that LBPA is in vesicles inside the erythrocyte-containing phagosome (Fig. 7 Zoom). CTCF quantification showed that LBPA diminished 36% from steady state conditions to 15 min of phagocytosis, but then, at 60 and 90 min it increased to 72.9% more than in steady state conditions (Fig. 7B). Besides, the relationship between LPBA labeled erythrocytes and total ingested erythrocytes showed that the number of labeled erythrocytes increased 1.72 fold, from 49.7% at 15 min to 85.7%, at 90 min (Fig. 7C). Altogether, these results make clear that an increment of LBPA inside phagosomes happened after 15 min of phagocytosis. Based on these results, it can be suggested that LBPA forms part of trophozoite phagosomes and lysophagosomes, as it has been reported for other systems [30,56,57].

3.6. Association of LBPA with EhRab7A protein

Discovering of membrane-molecules interactions is important for understanding the mechanisms underlying pinocytosis and phagocytosis. Uncovering of novel molecules and detection of their interaction sites can be useful for therapeutic intervention. In mammals, Rab7 GTPase participates in the regulation of trafficking of endosomes to late endosomes, lyososomes and phagosomes, and it is considered as a marker of late endosomes [58]. *E. histolytica* encodes several Rab7 proteins. EhRab7A has been found in phagosomes after 30 min of phagocytosis [7]. Accordingly to Saito-Nakano et al., it participates in maturation of late endosomes and in receptors recycling from phagosomes to the trans-Golgi network [7]. To determine the association of LBPA of *E. histolytica* with EhRab7A during erythrophagocytosis, we performed co-localizing experiments using 6C4 and anti-EhRab7A antibodies (Fig. 8). In steady state conditions, we found LBPA and EhRab7 in small vacuoles (Fig. 8). Then, throughout erythrophagocytosis, association between the protein and the phospholipid increased, mainly around ingested erythrocytes and in the huge erythrocytes-containing phagosomes that could correspond to MVBs and were also observed in Fig. 7. Accordingly to Saito-Nakano et al., [7], EhRab7A-containing vesicles carry lysosomal enzymes to the phagosome.

3.7. LBPA is in acidic vesicles and it interacts with EhADH protein

LBPA is in acidic vesicles with a 5.5 pH [28,30] and it interacts with Alix protein during endocytosis and vesicular traffic [28,43].

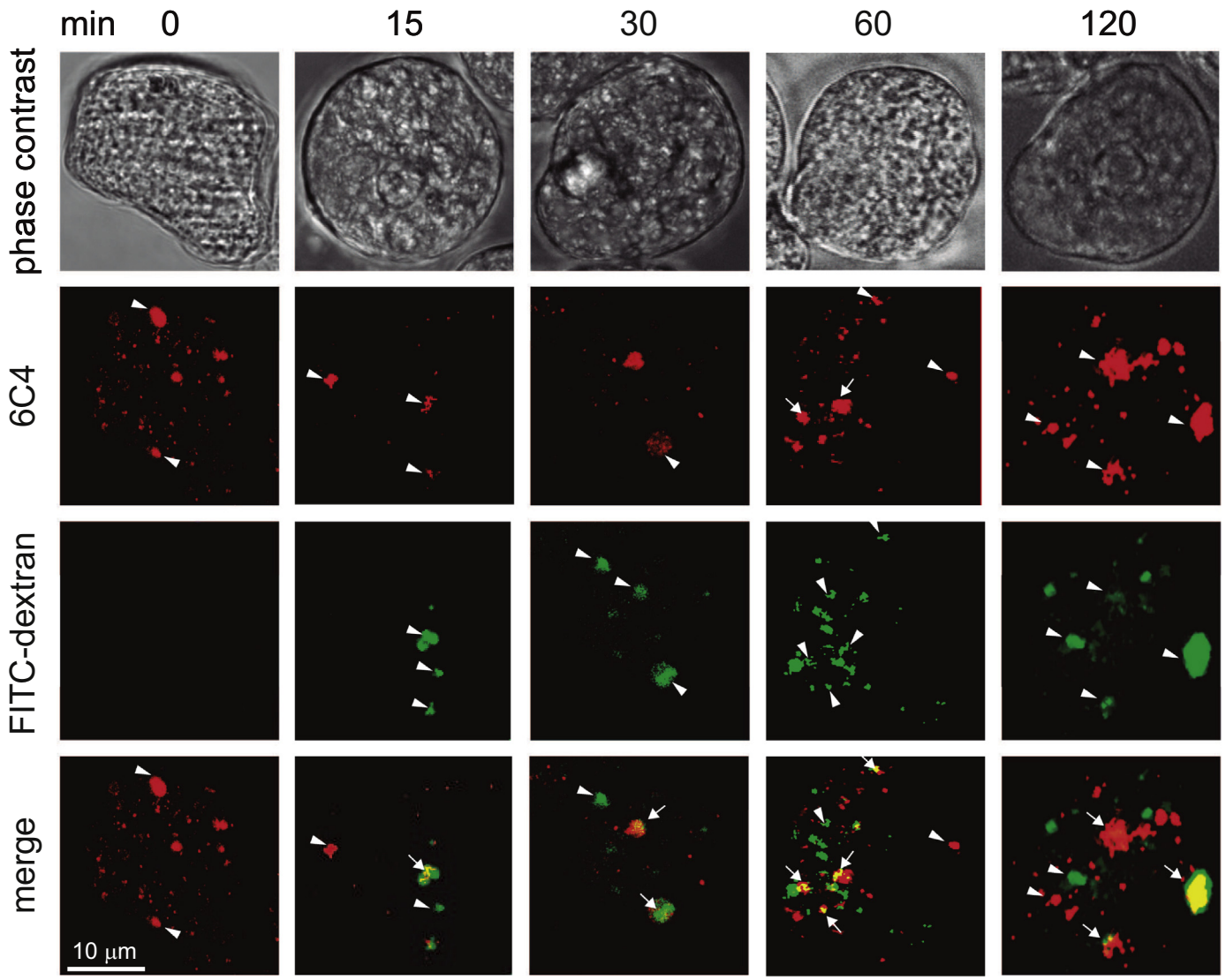

Fig. 4. Immunolocalization of LBPA during pinocytosis of FITC-dextran. Confocal microscopy images of trophozoites incubated at 37 °C with FITC-dextran for different times. LBPA was detected by 6C4 antibody and Alexa-594 secondary antibody. Arrows: Co-localization of LBPA and ingested particles. Arrowheads: LBPA (red) and FITC-dextran (green) stained vesicles. (For interpretation of the references to color in this figure legend, the reader is referred to the web version of this article.)

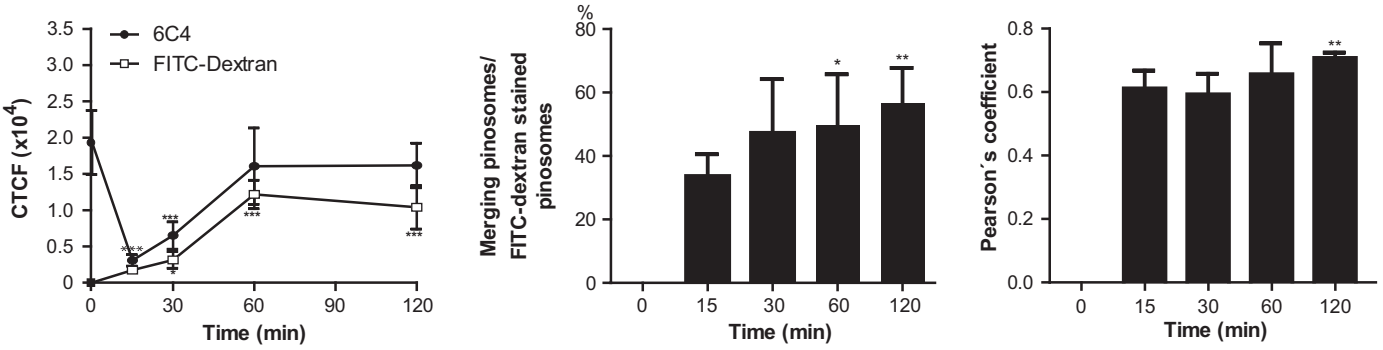

Fig. 5. Quantification of 6C4 antibody and FITC-dextran fluorescence during pinocytosis. Laser sections (1-μm Z-stack, $n=150$) from confocal images analyzed using Image J 1.48i software to measure: (A) whole cell fluorescence measuring 6C4 antibody or FITC-dextran after pinocytosis for different times: CTCF: corrected total cell fluorescence. (B) Relative percentage of merging vesicles. (C) Pearson´s coefficients quantified in merging stained vesicles at indicated times. Data are means ± standard deviation. (*): $p<0.051$, (**): $p<0.01$.

In *E.* histolytica, EhADH acts as a receptor for erythrocytes during phagocytosis and it also participates in endosomes formation, interacting with EhVps32 protein [59]. We investigated the nature of LBPA-containing vesicles and the interaction of LBPA with EhADH using Lysotracker Red and anti-EhADH antibodies. Confocal images showed that in steady state trophozoites, LBPA co-localizes with Lysotracker Red and EhADH (Fig. 9). EhADH protein was found in the plasma membrane and in the cytoplasm, as described

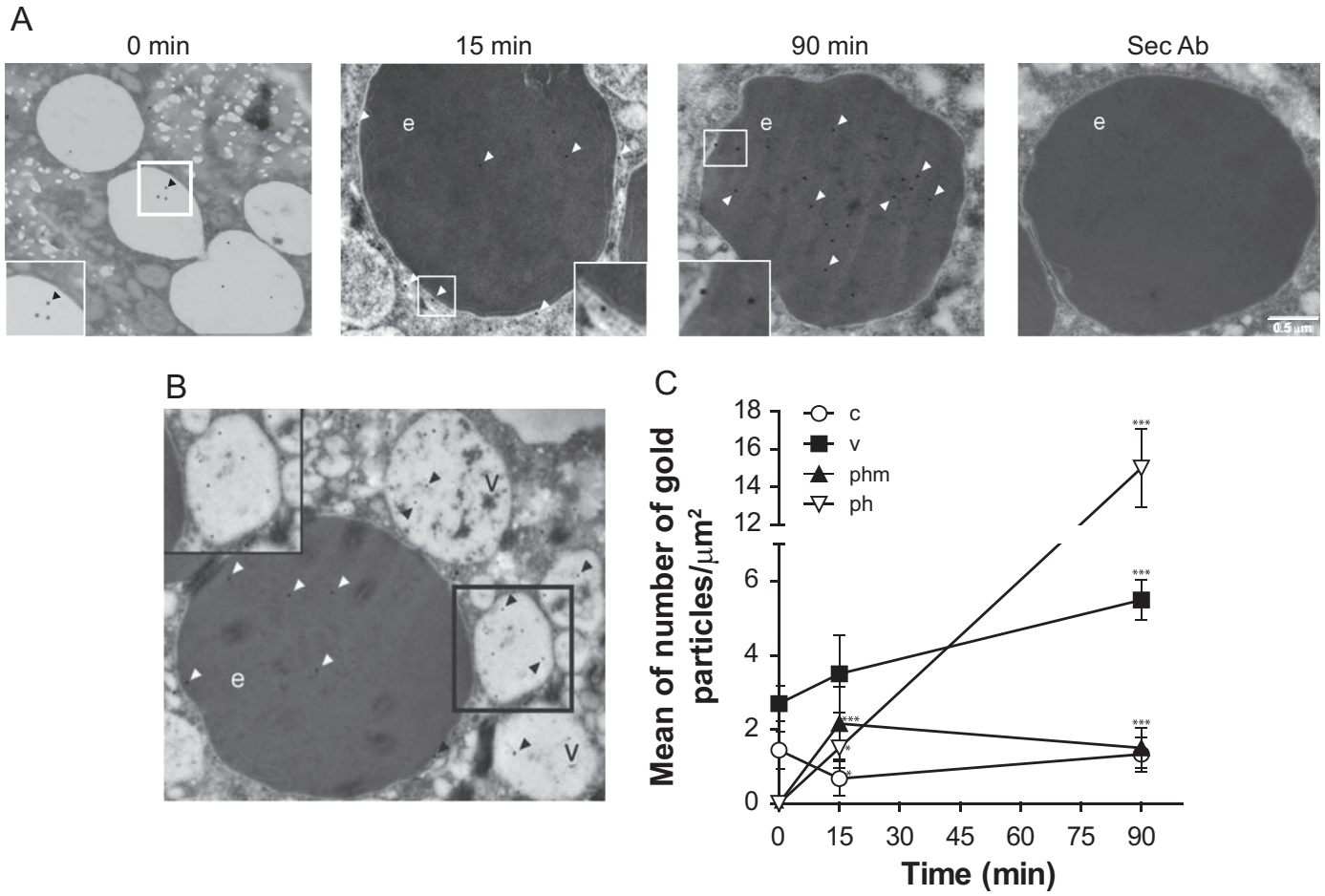

Fig. 6. TEM immunolocalization of LBPA during erythrophagocytosis. LBPA was localized using 6C4 antibody and gold-labeled secondary antibody on thin sections of trophozoites. (A) Ingested erythrocytes by trophozoites during erythrophagocytosis from 0 to 90 min. Sec Ab: assays performed using only secondary antibody. (B) Vacuoles around erythrocytes after 90 min phagocytosis. Arrowheads: Gold particles; v- vesicles; e: erythrocytes. Squares are magnified areas marked at bottom (A) and upper (B) squares. (C) Quantification of gold particles during phagocytosis. v: vesicles; c: cytoplasm; phm: phagosome membrane; ph: phagosome. Data are means ± standard deviation. (*): $p < 0.05$, (***): $p < 0.001$.

[10]. During phagocytosis, EhADH was also found in acidic vesicles, co-localizing with LBPA and Lysotracker. LBPA and EhADH appeared in phagosomes and around some ingested erythrocytes, as well as in erythrocytes-containing phagosomes, including the huge phagosomes that could correspond to MVBs (Fig. 9). Trophozoites, in steady state conditions, exhibited 72.6% of vesicles decorated by LBPA and Lysotracker and they increased to 87% after 60 and 90 min of phagocytosis. Their molecular association according to Pearson´s coefficient [51] was 0.77. However, Lysotracker was also found in 27.4 to 13% vesicles without LBPA (Fig. 10A), indicating that the majority LBPA containing vesicles are acidic, as it occurs in other systems [27]. Results also exhibited the different composition of endosomes, whereas some of them were stained only by anti-EhADH antibodies, other were decorated by 6C4 antibody or Lysotracker, while others appeared illuminated by both antibodies, and others more, by both antibodies and Lysotracker (Fig. 10B,C).

To further demonstrate the interaction between LBPA and EhADH, we performed immunoprecipitation assays using lysates from steady state trophozoites and from trophozoites that were incubated with erythrocytes for 90 min. Anti-EhADH and 6C4 antibodies were used to produce independent immunoprecipitates that were revealed in dot blot assays. Anti-EhADH and 6C4 antibodies recognized both immunoprecipitates (Fig. 11A,B). In western blot assays using these immunoprecipitates, anti-EhADH antibody recognized EhADH (75 kDa) and the EhCPADH complex (124 kDa), as described [10]. Immunoprecipitates produced using erythrocyte lysates gave negative results with anti-EhADH and 6C4 antibodies, as well as with pre-immune serum and with lecithin (Fig. 11A, B, and D). 6C4 antibody did not recognized erythrocytes, in agreement with other studies on phagocytosis using 6C4 antibody and erythrocytes [57]. In addition, anti-EhADH antibody did not recognize phospholipids spotted on the same membrane, neither LBPA standard (Fig. 10C). These results confirmed that LBPA interacted with EhADH at steady state conditions and during phagocytosis and suggested that LBPA and EhADH might be associated in phagosomes and in MVBs.

4. Discussion

During endocytosis, *E. histolytica* trophozoites present a dynamic membrane remodeling. LBPA has been described in other systems [34,38] as a fundamental compound in this event [60], among other functions of this phospholipid. Here, we identified, for the first time, six LBPA molecular species in *E. histolytica* trophozoites. Besides, we disclosed its presence in pinosomes and phagosomes during pinocytosis and phagocytosis, respectively. It associates with EhRab7 and EhADH, an ALIX family protein involved in phagocytosis. Interestingly, docking analysis suggested that the binding site of EhADH with LBPA is conserved [61] (Data

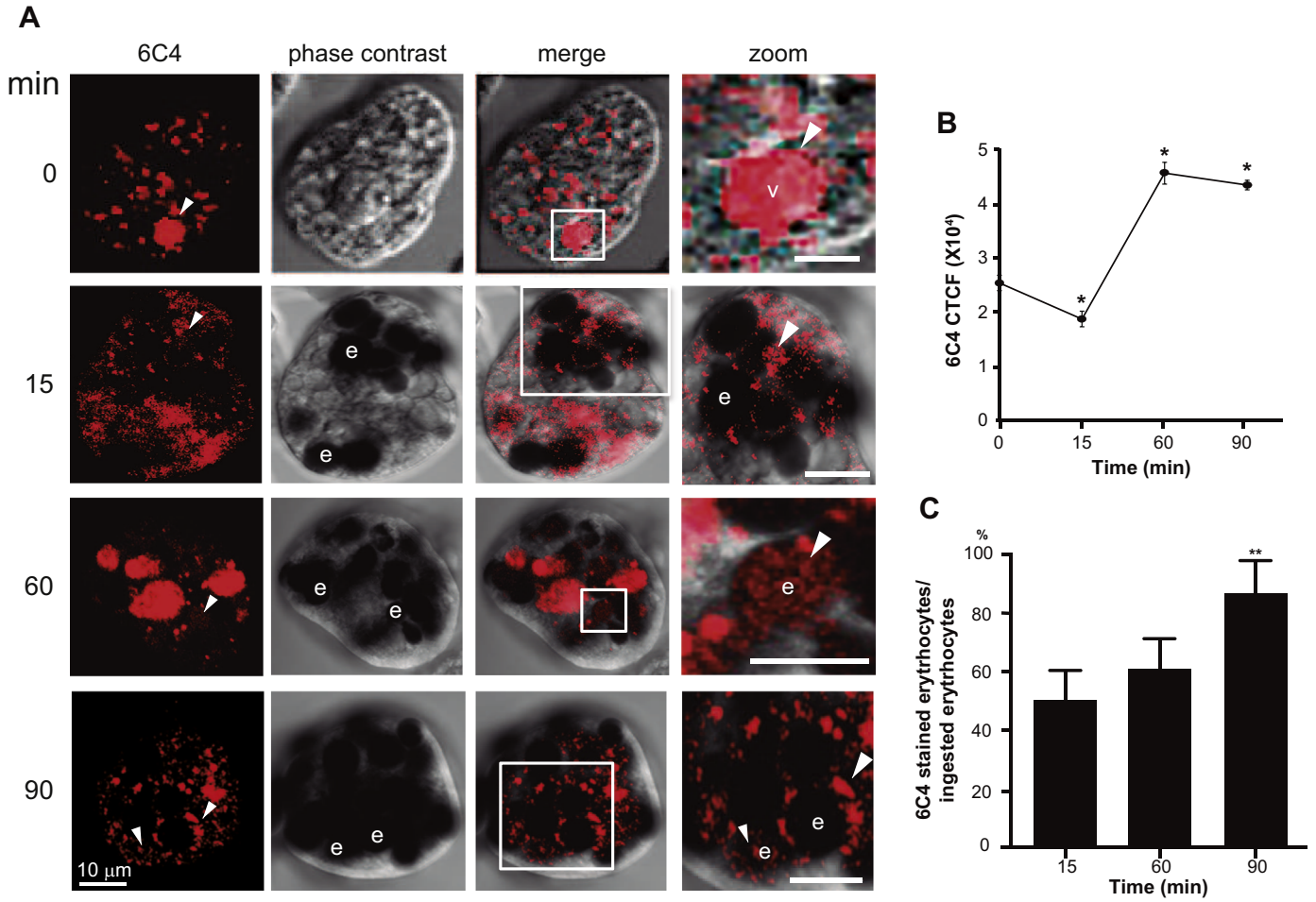

Fig. 7. Confocal microscopy images of LBPA during erythrophagocytosis. (A) Trophozoites were analyzed after 0–90 min erythrophagocytosis using 6C4 and Alexa 594 secondary antibodies. Zoom shows a magnification of LBPA in vacuoles and in and on erythrocytes-containing phagosomes. v: vacuoles, e: erythrocytes. Arrowheads: 6C4 stained vesicles and erythrocytes-containing phagosomes. (B) CTCF: corrected total cell fluorescence of 6C4 antibody. (C) Relative percentage of stained phagosomes. Data are means ± standard deviation. (*): $p < 0.05$, (***): $p < 0.001$.

in brief, submitted) in comparison with that detected in other Alix proteins [43].

In addition to mammalian cells, LBPA has been found in bacteria, by biochemical procedures [62]; in membrane lysosomes of *Dictyostelium discoideum*, using TLC [63]; and also, in *Leishmania Mexicana*-containing phagosomes of macrophages infected with this parasite, using 6C4 antibody [56]. In eukaryotes, LBPA takes part in the formation of endosome membrane domains to facilitate the sorting of molecules to be recycled or degraded. Although it composes 17% of the cell phospholipids, it is enriched in 70% in ILVs of late endosomes [30], thus, LBPA is considered as a marker of late phases of endocytosis [30].

Aley et al. [19] reported the presence of an unidentified lipid in total lipids of *E. histolytica* trophozoites, which they marked as "X" in two dimension TLC experiments. The "X" compound has a similar migration than LBPA of BHK cells [30], thus, it could correspond to *E. histolytica* LBPA detected here (Fig. 1). However, Aley et al., identified the "X" compound during the study of membrane phospholipids; and we detected LBPA using the 6C4 antibody. The use of distinct methodology maintains an open question on whether "X" compound correspond to *E. histolytica* LBPA.

The 6C4 monoclonal antibody generated by Kobayashi et al. [38] resulted to be an excellent tool for LBPA identification in *E. histolytica* trophozoites. Recognition of LBPA in trophozoites by this antibody was highly specific and dose-response dependent. It did not react with proteins or other lipids such as other TLC-revealed spots, as it was shown in dot blot experiments (Fig. 1). It did not react with erythrocytes as shown by immunofluorescence and dot blot assays in Fig. 11C and D. HPLC coupled to mass spectrometry assays using (*S*,*S*)-2,2-bisoleoyl-LBPA as standard, allowed us to confirm that the molecule recognized by the 6C4 antibody in *E. histolytica* trophozoites was indeed LBPA. Ion fragmentation confirmed the nature of the lipid recognized by 6C4 antibodies (Fig. 2). Phosphatydilglycerol (PG) has been described as LBPA structural isomer with similar molecular weight. However, Mortuza et al. [34] reported that PG retention time is approximately seven minutes shorter than the one of LBPA. Thus, we used the methodology described by Mortuza et al. [34] to accurately separate *E. histolytica* LBPA and determine its molecular species. *E. histolytica* has at least two LBPA groups with three distinct molecular species each one; however, our experiments did not discard the existence of other ions that were not detected by this approach (Fig. 2). LBPA species presented a relative abundance of polyunsaturated fatty acid chains, being the major ion a 38:3 (18:1/20:2*)* molecule. This characteristic may confer to trophozoite membranes a higher possibility to form curved domains, necessary for vesicle fusion and fission, as reported for other eukaryotes [28]. In addition, liposomes composed by (*S, S*)-2,2´-bisoleoyl-LBPA spontaneously formed multivesicular liposomes depending on pH [28]. This biophysical property has been related to the curved membranes formation and membrane flexibility (24, 25) and, therefore, necessary for ILVs generation.

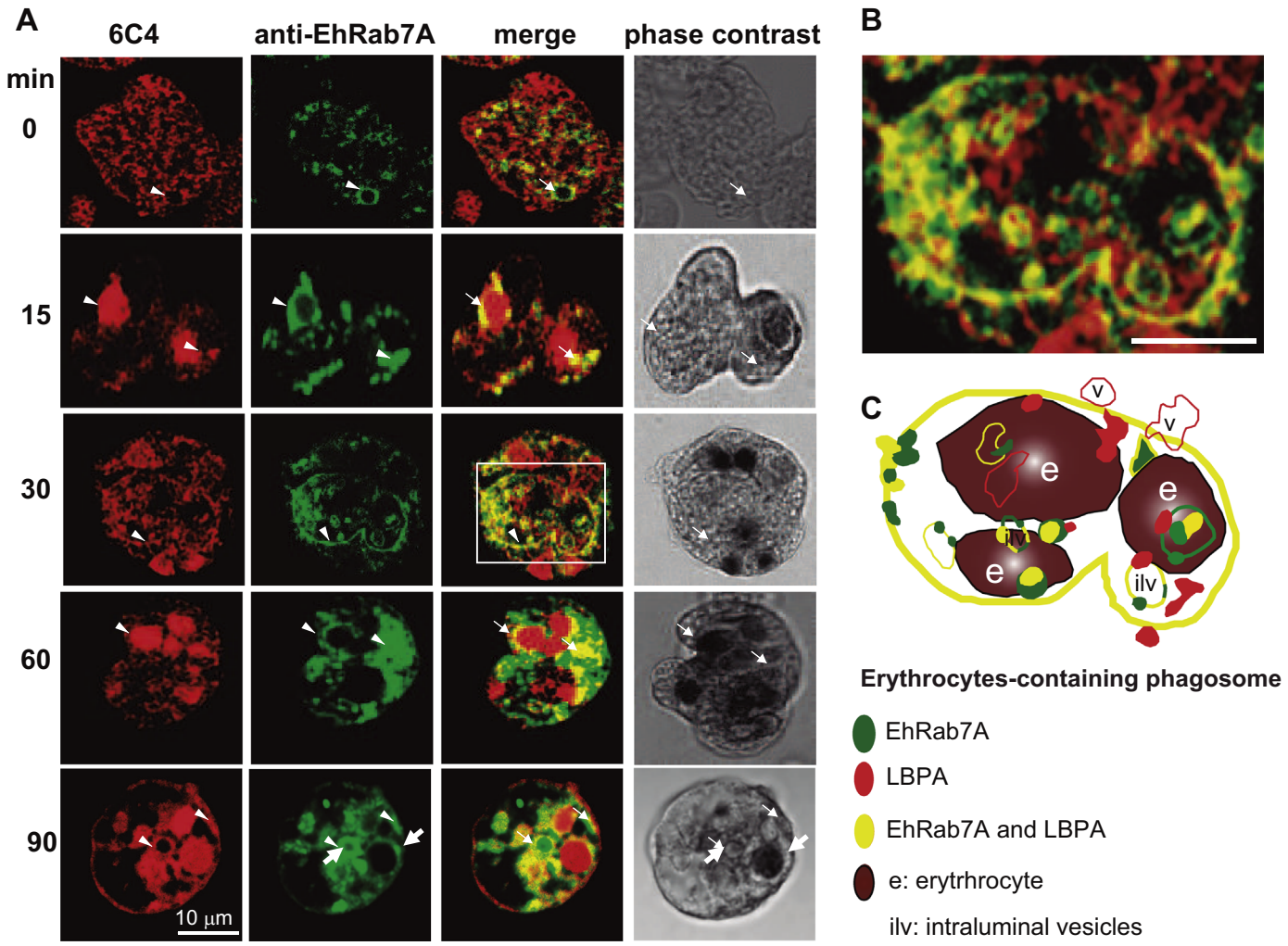

Fig. 8. Co-localization of LBPA and EhRab7A protein during erythrophagocytosis. Trophozoites incubated with erythrocytes from 0 to 90 min were double stained by 6C4 and anti-EhRab7A antibodies followed by Alexa 594 and FITC secondary antibodies, respectively. Arrowheads: labeled cellular structures. Arrows: Co-localization in vesicles, erythrocytes and phagosomes.

Most of the cells studied have several LBPA molecular species. Fatty acid composition of LBPA has a high proportion of unsaturated and polyunsaturated acyl chains, being the most abundant the oleic acid (18:1) [30,33,34,54]. LC-ESI-MS assays allowed us to unveil, in *E. histolytica* trophozoites, the asymmetric 18:1/20:2 ion as the most abundant LBPA molecular species. Additionally, the 18:1 fatty acid chain has 92% of relative abundance among LBPA molecular species detected here (Table 1). We have not studied in this work what is the significance of the presence of distinct LBPA molecular species in trophozoites. However, we can hypothesize that a mixture of them could account for membrane flexibility in trophozoites, which present distinct vital functions in which membrane remodeling is necessary, such as phagocytosis, pinocytosis, pseudopodia emission, motility, cellular division, among others. This property is basic for other functions related with endocytosis, such as MVBs and ILVs production and transport of distinct molecules. Other LBPA molecular species could participate in EhRab7A, EhADH and other proteins binding as well as in cholesterol transport to recruit them at the endosome membranes. In mammals, 2-2´-bisoleoyl-LBPA participates in cholesterol transport [64]. *E. histolytica* trophozoites take cholesterol from the medium, because they have no the machinery to synthesize it, but inside the cell, cholesterol must be sorted to distinct organelles. As in other eukaryotes, *E. histolytica* LBPA esterified with 18:1 fatty acid chain could be involved in cholesterol transport. Besides these putative functions and other mentioned above, LBPA molecular species may have a role as donor and acceptor of fatty acid chains to be exchanged with other types of phospholipids [54].

As in mammalian cells [37], *E. histolytica* LBPA was found in acid vesicles and in ILVs of late, endosomes (Figs. 7–9). Furthermore, it appeared in vacuoles in steady state conditions and during dextran uptake and erythrophagocytosis (Figs. 4 and 7). Thus, in addition to its association to endosomes, LBPA could be involved in other steps of the process, or it may be participating in other functions such as the ones discussed above. Its detection in steady state trophozoites may be due to the high basal endocytosis activity of trophozoites.

Surprisingly, CTCF assays showed, after 15 min pinocytosis that LBPA diminished 6–7 fold, and then, after 60 min it increased to reach the steady state concentration (Fig. 5). Macrophages, also present a lower percentage of LBPA (related to total lipids) when they are activated by BSG protein (4.1%), than when they are in resting conditions (18.6%) [54]. According to Cochran et al. [54], LBPA is the phospholipid with the greatest changes upon macrophage activation. Immediately after activation, the pool of certain lipids, including LBPA, is used by macrophages to synthesize other metabolites, functioning as acceptors or donors of fatty acid chains [54]. In *E. histolytica* trophozoites, it is possible that, even when dextran uptake is not receptor mediated, trophozoites could sense the presence of the compound because dextran is accumulated in

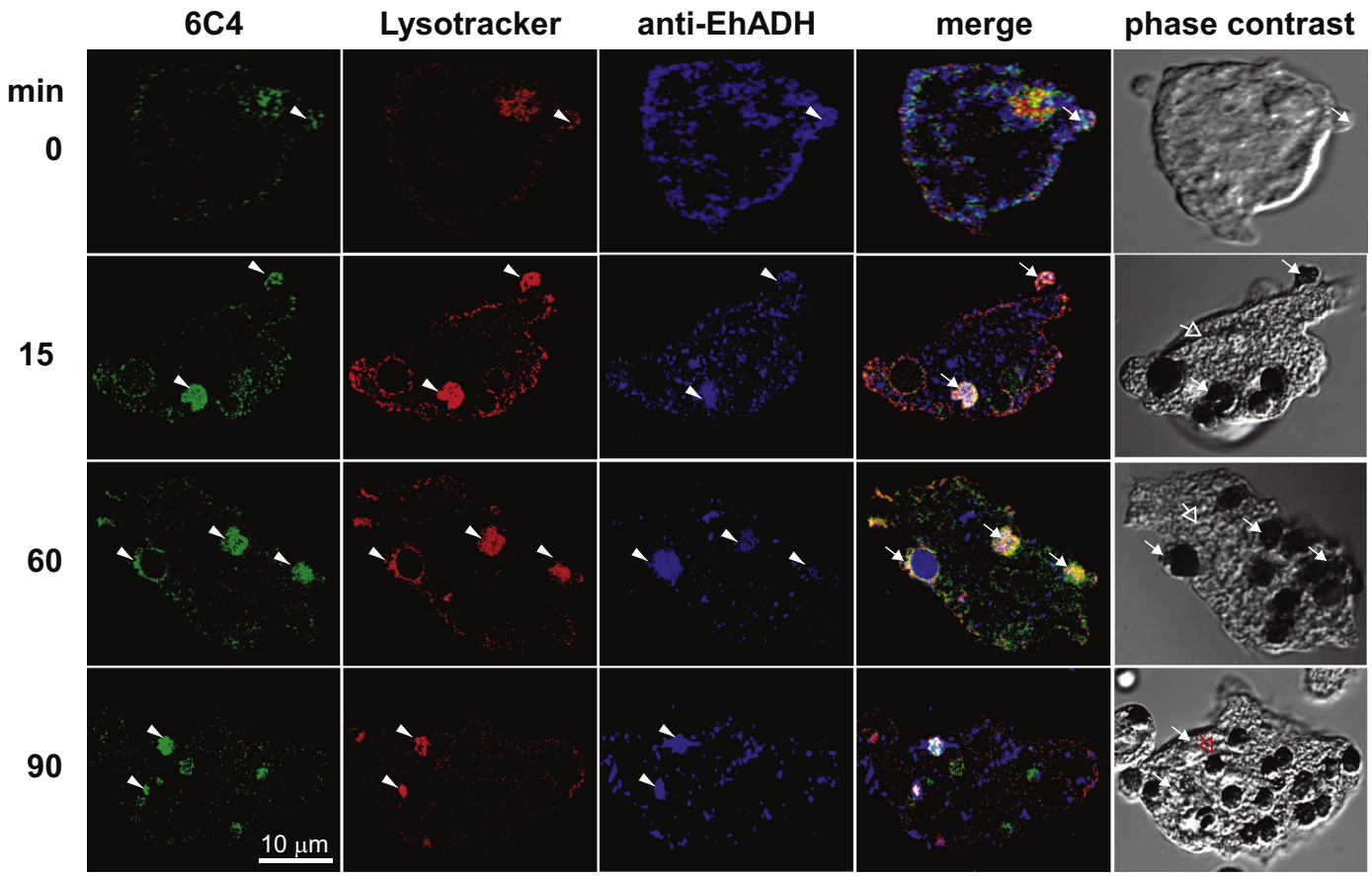

Fig. 9. Co-localization of LBPA, EhADH protein and Lysotracker during erythrophagocytosis. Trophozoites incubated with erythrocytes from 0 to 90 min were triple stained by 6C4 and anti-EhRab7A antibodies followed by Alexa 594 and FITC secondary antibodies, respectively and Lysotracker. Arrowheads: labeled cellular structures. Arrows: Co-localization in vesicles, erythrocytes and phagosomes.

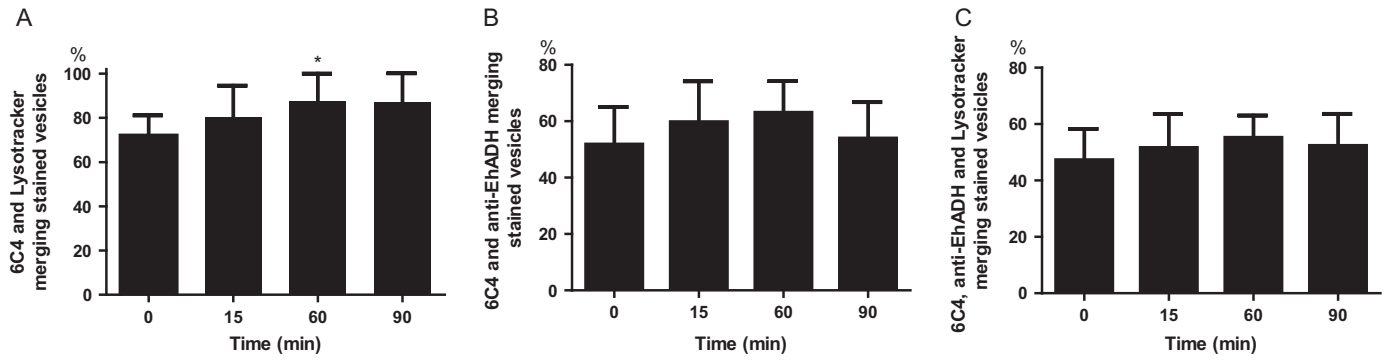

Fig. 10. Quantification of 6C4, anti-EhADH antibodies and Lysotracker stained vesicles in trophozoites during phagocytosis. Laser sections (1-μm Z-stack, $n=150$) from confocal images were analyzed using Image J 1.48i to measure: (A–C) Relative percentage of merging vesicles as indicated in *Y*-axis. Data are means ± standard deviation. (*): $p < 0.01$.

large vesicles by macropinocytosis [65]. As a response to this stimulus they could synthesis and degrade distinct molecules. This hypothesis could explain why in the beginning of the dextran uptake process LBPA diminished, and then, the phospholipid presented similar amount of fluorescence to the one registered at steady state levels.

The drop in LBPA concentration after 15 min of phagocytosis was less dramatic than in pinocytosis. The participation of LBPA in both pathways should be different. Phagocytosis is a receptor-mediated event that conducts cell to synthesis and degrade certain metabolites. On the other hand, pinocytosis does not involve membrane receptors, thus, metabolites needed for this event may differ from the ones required for phagocytosis. After 60 min of phagocytosis, LBPA concentration increased 60% in comparison with 0 time; and it was precisely after 60 min phagocytosis that vesicles in trophozoites appeared larger and brighter (Figs. 7 and 8). Coincidently, at 90 min, the number of gold particles detecting LBPA also increased 11 fold, according to TEM experiments (Fig. 6). In mammalian cells, LBPA participates in distribution of cargo molecules to lysosomes or Golgi apparatus [66]. Golgi apparatus in *E. histolytica* is not completely characterized, however, Saito-Nakano et al., [7] found that EhRab7A protein is involved in vesicular trafficking after 30 min of phagocytosis and it controls late endosomes to Golgi transport. Also, the number of 6C4 stained phagosomes of smooth muscle cells increased after 30 and 45 min of erythrophagocytosis indicating phagosome maturation [57].

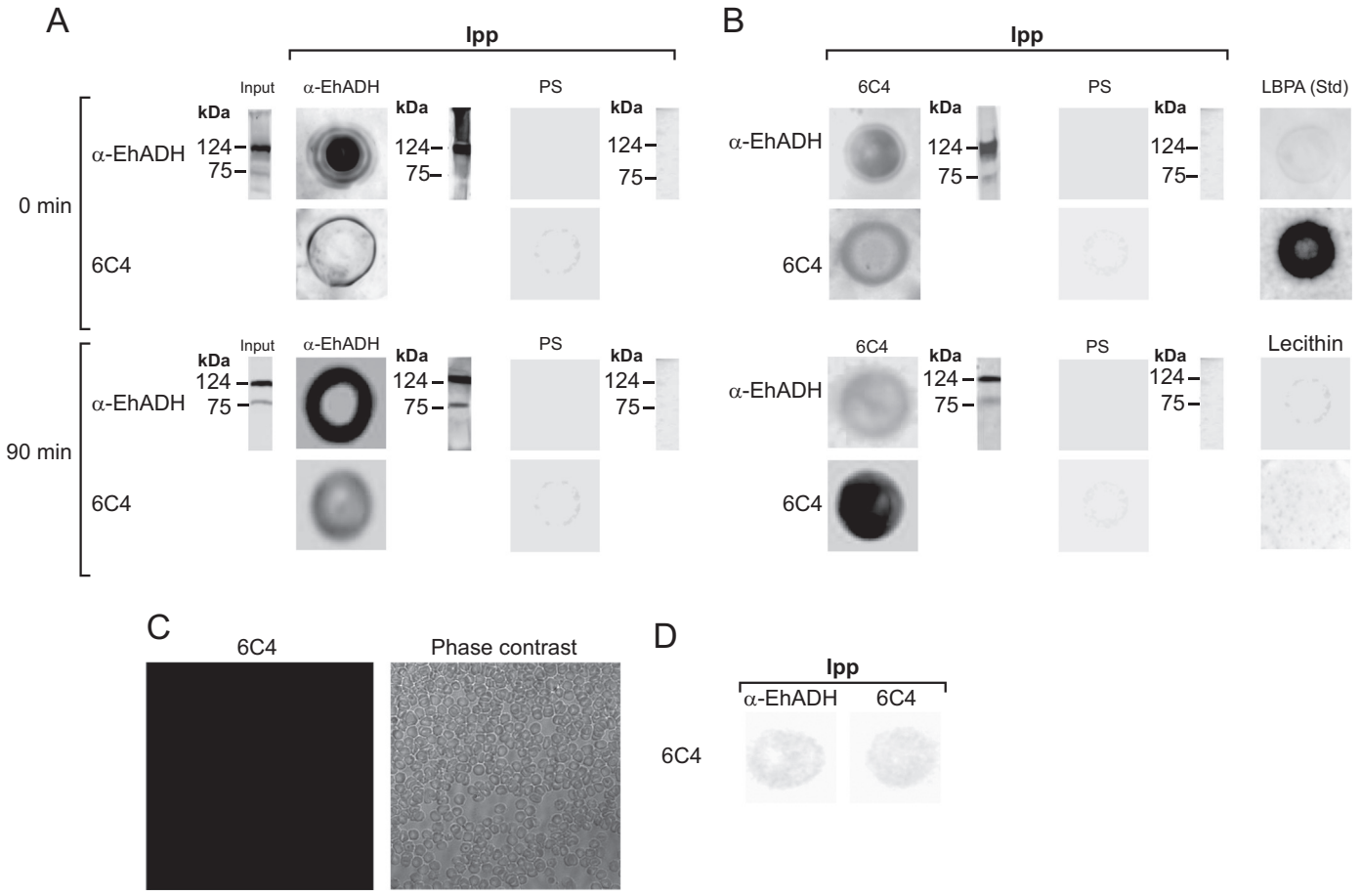

Fig. 11. Interaction of *E. histolytica* LBPA and EhADH in steady state condition and during phagocytosis. Total proteins from trophozoites in basal conditions and after 90 min of incubation with Ficoll purified and hemoglobin depleted erythrocytes were incubated with (A) anti-EhADH, (B) 6C4 antibody, or (PS) pre-immune serum. Immunoprecipitated samples were spotted on nitrocellulose membranes and dot blot assays were performed using anti-EhADH and 6C4 antibodies. At the right and left of dot blots and input, respectively, are the western blots of immunoprecipitates, using anti-EhADH antibody. LBPA: (*S,S*)-2,2′-bisoleoyl-LBPA standard and lecithin were spotted on PVDF membranes revealed with 6C4 antibody and anti-EhADH. (C) Control. Erythrocytes stained with 6C4 antibody of fixed and permeabilized erythrocytes and examined under confocal microscope. (D) Immunoprecipitation of erythrocytes lysates treated with anti-EhADH and 6C4 antibodies and revealed with 6C4.

Furthermore, it has been stated that in trophozoites, the digestion starts after 90 min of phagocytosis [67], thus, it is possible to hypothesize that LBPA could contribute in transport and recycling of certain molecules.

The finding of LBPA associated or interacting with EhRab7A and EhADH in huge phagosomes, containing many ILVs, strengthens the hypothesis that these molecules are involved in late endosomes formation and function. In mammalian cells, LBPA and Alix protein are associated during late endocytosis [28] and virus penetration to host cells [43]. Alix Bro1 domain, located at the *N*-terminus of these proteins mediates this association [43]. Similarly, in *E. histolytica* EhADH functions as a receptor for erythrocytes. Additionally, both molecules participate in cholesterol distribution and in sorting of cargo particles that will be recycled or delivered to lysosomes. In *E. histolytica*, LBPA and EhADH interact in resting trophozoites and throughout phagocytosis pathway, as it has been demonstrated by immunofluorescence and immunoprecipitation assays (Figs. 9 and 11). Association of both molecules in resting trophozoites could be related to the very active endocytosis that trophozoites have during steady state, or it may be explained by their involvement in a distinct function, such as cholesterol transport.

5. Conclusions

LBPA was biologically and structurally characterized in *E. histolytica* trophozoites. TLC and LC-ESI-MS experiments revealed that LBPA is represented by at least six molecular species rich in unsaturated acyl chains. It associates with pinosomes and phagosomes; and it is found in ILV's in phagosomes and MVBs. Additionally, we presented experimental evidences of phospholipid-protein association and interaction between LBPA and EhRab7A and EhADH, respectively.

Acknowledgments

We are grateful to Dr. Tomoyoshi Nosaki (National Institute of Infectious Diseases, Toyama, Shinjuku-ku, Tokyo, Japan) and Dr. Lesly Temesvari (Clemson University, Ca USA) for kindly given us the anti-EhRab antibodies. We are grateful to the Unit of Confocal Microscopy and Unit of Genomics, Proteomics and Metabolomics of Central Laboratories of CINVESTAV for their help with HPLC and Mass Spectrometry assays and to Alfredo Padilla Barberi for art work, to Patricia Cuellar for preparing the anti-EhADH antibody and to Dr. Abigail Betanzos for critical reading of the manuscript. Conacyt and CINVESTAV-IPN provided financial support. Silvia Castellanos Castro received a fellowship from Conacyt.

Appendix A. Transparency Document

Transparency Document associated with this article can be found in the online version at http://dx.doi.org/10.1016/j.bbrep.2015.12.010.

References

[1] V. Zermeno, et al., Worldwide genealogy of *Entamoeba histolytica*: an overview to understand haplotype distribution and infection outcome, Infect. Genet. Evol. 17 (2013) 243–252.
[2] H. Tachibana, et al., Characterization of *Entamoeba histolytica* intermediate subunit lectin-specific human monoclonal antibodies generated in transgenic mice expressing human immunoglobulin loci, Infect. Immun. 77 (1) (2009) 549–556.
[3] S. Somlata, Bhattacharya, A. Bhattacharya, A C2 domain protein kinase initiates phagocytosis in the protozoan parasite *Entamoeba histolytica*, Nat. Commun. 2 (2011) 230.
[4] M.S. Mansuri, S. Bhattacharya, A. Bhattacharya, A novel alpha kinase EhAK1 phosphorylates actin and regulates phagocytosis in *Entamoeba histolytica*, Plos Pathog. 10 (10) (2014), p. e1004411.
[5] B.H. Welter, R.C. Laughlin, L.A. Temesvari, Characterization of a Rab7-like GTPase, EhRab7: a marker for the early stages of endocytosis in *Entamoeba histolytica*, Mol. Biochem. Parasitol. 121 (2) (2002) 254–264.
[6] Y. Saito-Nakano, et al., Rab5-associated vacuoles play a unique role in phagocytosis of the enteric protozoan parasite *Entamoeba histolytica*, J. Biol. Chem. 279 (47) (2004) 49497–49507.
[7] Y. Saito-Nakano, et al., Two Rab7 isotypes, EhRab7A and EhRab7B, play distinct roles in biogenesis of lysosomes and phagosomes in the enteric protozoan parasite *Entamoeba histolytica*, Cell. Microbiol. 9 (7) (2007) 1796–1808.
[8] Y. Saito-Nakano, et al., The diversity of Rab GTPases in *Entamoeba histolytica*, Exp. Parasitol. 110 (3) (2005) 244–252.
[9] M.A. Rodriguez, E. Orozco, Characterization of the EhRabB recombinant protein of *Entamoeba histolytica*, Arch. Med. Res. 31 (Suppl 4) (2000) S171–S172.
[10] G. García-Rivera, et al., *Entamoeba histolytica*: a novel cysteine protease and an adhesin form the 112 kDa surface protein, Mol. Microbiol. 33 (3) (1999) 556–568.
[11] C. Bañuelos, et al., Functional characterization of EhADH112: an *Entamoeba histolytica* Bro1 domain-containing protein, Exp. Parasitol. 110 (3) (2005) 292–297.
[12] C. Banuelos, et al., EhADH112 is a Bro1 domain-containing protein involved in the *Entamoeba histolytica* multivesicular bodies pathway, J. Biomed. Biotechnol. 2012 (2012) 657942.
[13] J. Cerbon, J. Flores, Phospholipid composition and turnover of pathogenic amebas, Comp. Biochem. Physiol. 69B (1981) 487–492.
[14] J. Andra, O. Berninghausen, M. Leippe, Membrane lipid composition protects *Entamoeba histolytica* from self-destruction by its pore-forming toxins, FEBS Lett. 564 (1–2) (2004) 109–115.
[15] Y.A. Byekova, et al., Localization of phosphatidylinositol (3,4,5)-trisphosphate to phagosomes in entamoeba histolytica achieved using glutathione S-transferase- and green fluorescent protein-tagged lipid biosensors, Infect. Immun. 78 (1) (2010) 125–137.
[16] R.R. Powell, et al., Entamoeba histolytica: FYVE-finger domains, phosphatidylinositol 3-phosphate biosensors, associate with phagosomes but not fluid filled endosomes, Exp. Parasitol. 112 (4) (2006) 221–231.
[17] A. Olivos, et al., Entamoeba histolytica: mechanism of decrease of virulence of axenic cultures maintained for prolonged periods, Exp. Parasitol. 110 (3) (2005) 309–312.
[18] J. Serrano-Luna, et al., Effect of phosphatidylcholine-cholesterol liposomes on *Entamoeba histolytica* virulence, Can. J. Microbiol. 56 (12) (2010) 987–995.
[19] S.B. Aley, W.A. Scott, Z.A. Cohn, Plasma membrane of *Entamoeba histolytica*, J. Exp. Med. 152 (2) (1980) 391–404.
[20] F.G. van der Goot, J. Gruenberg, Intra-endosomal membrane traffic, Trends Cell. Biol. 16 (10) (2006) 514–521.
[21] J. Gruenberg, The endocytic pathway: a mosaic of domains, Nat. Rev. Mol. Cell. Biol. 2 (10) (2001) 721–730.
[22] J. Gruenberg, Lipids in endocytic membrane transport and sorting, Curr. Opin. Cell. Biol. 15 (4) (2003) 382–388.
[23] K. Bowers, et al., Protein–protein interactions of ESCRT complexes in the yeast Saccharomyces cerevisiae, Traffic 5 (3) (2004) 194–210.
[24] M. Babst, et al., The Vps4p AAA ATPase regulates membrane association of a Vps protein complex required for normal endosome function, EMBO J. 17 (1998) 2982–2993.
[25] M. Zerial, H. McBride, Rab proteins as membrane organizers, Nat. Rev. Mol. Cell. Biol. 2 (2) (2001) 107–117.
[26] S. Friant, et al., Ent3p Is a PtdIns(3,5)P2 effector required for protein sorting to the multivesicular body, Dev. Cell. 5 (3) (2003) 499–511.
[27] W. Mobius, et al., Recycling compartments and the internal vesicles of multivesicular bodies harbor most of the cholesterol found in the endocytic pathway, Traffic 4 (4) (2003) 222–231.
[28] H. Matsuo, et al., Role of LBPA and Alix in multivesicular liposome formation and endosome organization, Science 303 (5657) (2004) 531–534.
[29] I. Dikic, ALIX-ing phospholipids with endosome biogenesis, Bioessays 26 (6) (2004) 604–607.
[30] T. Kobayashi, et al., Separation and characterization of late endosomal membrane domains, J. Biol. Chem. 277 (35) (2002) 32157–32164.
[31] A. Goursot, et al., Structure, dynamics, and energetics of lysobisphosphatidic acid (LBPA) isomers, J. Phys. Chem. B 114 (47) (2010) 15712–15720.
[32] N. Besson, et al., Selective incorporation of docosahexaenoic acid into lysobisphosphatidic acid in cultured THP-1 macrophages, Lipids 41 (2) (2006) 189–196.
[33] R. Kakela, P. Somerharju, J. Tyynela, Analysis of phospholipid molecular species in brains from patients with infantile and juvenile neuronal-ceroid lipofuscinosis using liquid chromatography-electrospray ionization mass spectrometry, J. Neurochem. 84 (5) (2003) 1051–1065.
[34] G.B. Mortuza, et al., Characterisation of a potential biomarker of phospholipidosis from amiodarone-treated rats, Biochim. Biophys. Acta 1631 (2) (2003) 136–146.
[35] A. Joutti, et al., The stereochemical configuration of lysobisphosphatidic acid from rat liver, rabbit lung and pig lung, Biochim. Biophys. Acta 450 (2) (1976) 206–209.
[36] J. Brotherus, et al., Novel stereoconfiguration in lyso-bis-phosphatidic acid of cultured BHK-cells, Chem. Phys. Lipids 13 (2) (1974) 178–182.
[37] T. Kobayashi, et al., Late endosomal membranes rich in lysobisphosphatidic acid regulate cholesterol transport, Nat. Cell. Biol. 1 (2) (1999) 113–118.
[38] T. Kobayashi, et al., A lipid associated with the antiphospholipid syndrome regulates endosome structure and function, Nature 392 (6672) (1998) 193–197.
[39] T. Falguieres, P.P. Luyet, J. Gruenberg, Molecular assemblies and membrane domains in multivesicular endosome dynamics, Exp. Cell. Res. 315 (9) (2009) 1567–1573.
[40] I. Delton-Vandenbroucke, et al., Anti-bis(monoacylglycero)phosphate antibody accumulates acetylated LDL-derived cholesterol in cultured macrophages, J. Lipid Res. 48 (3) (2007) 543–552.
[41] Z. Chu, D.P. Witte, X. Qi, Saposin C-LBPA interaction in late-endosomes/lysosomes, Exp. Cell. Res. 303 (2) (2005) 300–307.
[42] T. Kolter, K. Sandhoff, Principles of lysosomal membrane digestion: stimulation of sphingolipid degradation by sphingolipid activator proteins and anionic lysosomal lipids, Annu. Rev. Cell. Dev. Biol. 21 (2005) 81–103.
[43] C. Bissig, et al., Viral infection controlled by a calcium-dependent lipid-binding module in ALIX, Dev. Cell. 25 (4) (2013) 364–373.
[44] L.S. Diamond, D.R. Harlow, C.C. Cunnick, A new medium for the axenic cultivation of *Entamoeba histolytica* and other Entamoeba, Trans. R. Soc. Trop. Med. Hyg. 72 (4) (1978) 431–432.
[45] J. Folch, M. Lees, G.H. Sloane Stanley, A simple method for the isolation and purification of total lipides from animal tissues, J. Biol. Chem. 226 (1) (1957) 497–509.
[46] B.N. Ames, Assay of inorganic phosphate, total phosphate and phosphatases, Methods Enzym. 8 (1966) 115–118.
[47] A.B. Novikoff, et al., Studies on microperoxisomes. II. A cytochemical method for light and electron microscopy, J. Histochem. Cytochem. 20 (12) (1972) 1006–1023.
[48] C.A. Schneider, W.S. Rasband, K.W. Eliceiri, NIH Image to ImageJ: 25 years of image analysis, Nat. Methods 9 (2012) 671–675.
[49] O. Gavet, J. Pines, Progressive activation of CyclinB1-Cdk1 coordinates entry to mitosis, Dev. Cell. 18 (4) (2010) 533–543.
[50] T.A. Potapova, et al., Mitotic progression becomes irreversible in prometaphase and collapses when Wee1 and Cdc25 are inhibited, Mol. Biol. Cell. 22 (8) (2011) 1191–1206.
[51] S. Bolte, F.P. Cordelieres, A guided tour into subcellular colocalization analysis in light microscopy, J. Microsc. 224 (Pt 3) (2006) 213–232.
[52] A.V. Chernyshev, et al., Erythrocyte lysis in isotonic solution of ammonium chloride: theoretical modeling and experimental verification, J. Theor. Biol. 251 (1) (2008) 93–107.
[53] C.G. Figdor, W.S. Bont, J.E. De Vries, Rapid isolation of mononuclear cells from buffy coats prepared by a new blood cell separator, J. Immunol. Methods 55 (2) (1982) 221–229.
[54] F.R. Cochran, et al., Regulation of arachidonic acid metabolism in resident and BCG-activated alveolar macrophages: role of lyso(bis)phosphatidic acid, J. Immunol. 138 (1987) 1877–1883.
[55] S.B. Aley, Z.A. Cohn, W.A. Scott, Endocytosis in *Entamoeba histolytica*. Evidence for a unique non-acidified compartment, J. Exp. Med. 160 (3) (1984) 724–737.
[56] U.E. Schaible, et al., Parasitophorous vacuoles of Leishmania mexicana acquire macromolecules from the, J. Cell. Sci. 112 (5) (1999) 681–693.
[57] M.S. Viegas, L.M. Estronca, O.V. Vieira, Comparison of the kinetics of maturation of phagosomes containing apoptotic cells and IgG-opsonized particles, Plos One 7 (10) (2012), p. e48391.
[58] P. Chavrier, et al., Localization of low molecular weight GTP binding proteins to exocytic and endocytic compartments, Cell 62 (2) (1990) 317–329.
[59] Y. Avalos-Padilla, et al., EhVps32 is a vacuole-associated protein involved in pinocytosis and phagocytosis of *Entamoeaba histolytica*, Plos Pathog. 11 (7) (2015), p. e1005079.
[60] F. Hullin-Matsuda, et al., Bis(monoacylglycero)phosphate, a peculiar phospholipid to control the fate of cholesterol: implications in pathology, Prostaglandins, Leukot. Essent. Fat. Acids 81 (5–6) (2009) 313–324.
[61] Castellanos-Castro Silvia, M.S.a.O.E., Docking and dynamics simulation of *Entamoeba histolytica* EhADH (an ALIX protein) and lysobisphosphatidic acid, Data in Brief, submitted, 2015.
[62] M. Nishihara, H. Morii, Y. Koga, Bis(monoacylglycero)phosphate in alkalophilic bacteria, J. Biochem. 92 (5) (1982) 1469–1479.
[63] J.M. Rodriguez-Paris, K.V. Nolta, T.L. Steck, Characterization of lysosomes isolated from Dictyostelium discoideum by magnetic fractionation, J. Biol. Chem. 268 (12) (1993) 9110–9116.
[64] J. Chevallier, et al., Lysobisphosphatidic acid controls endosomal cholesterol levels, J. Biol. Chem. 283 (41) (2008) 27871–27880.
[65] J.A. Swanson, C. Watts, Macropinocytosis, Trends Cell. Biol. 5 (11) (1995) 424–428.
[66] L.M. cBredeston, et al., Golgi and endoplasmic reticulum functions take place in different subcellular compartments of *Entamoeba histolytica*, J. Biol. Chem. 280 (37) (2005) 32168–32176.
[67] I. Meza, M. Clarke, Dynamics of endocytic traffic of *Entamoeba histolytica* revealed by confocal microscopy and flow cytometry, Cell. Motil. Cytoskelet. 59 (4) (2004) 215–226.